

Strip-Fed Rectangular Dielectric Resonator Antennas With/Without a Parasitic Patch

Bin Li, *Student Member, IEEE*, and Kwok Wa Leung, *Senior Member, IEEE*

Abstract—A rectangular dielectric resonator antenna (DRA) was studied theoretically and experimentally. The rectangular DRA is excited by a strip, which is compatible with a coaxial probe. Both linearly polarized (LP) and circularly polarized (CP) fields of the antenna are considered. In previous studies of the LP rectangular DRA, only the fundamental TE_{111} mode has received much attention. In this paper, it is found that the fundamental TE_{111} mode, together with the higher-order TE_{113} mode, can be used to design a wide-band LP DRA. The bandwidth of the dual-mode DRA can be over 40% for a conventional rectangular DRA with a simple feed. For the CP mode, a parasitic patch is attached on a side wall of the DRA to excite a degenerate mode. In both the LP and CP cases, the finite-difference time-domain (FDTD) method is used to analyze the problems. The results agree reasonably with measurements.

Index Terms—Circularly polarization, dielectric resonator antennas (DRAs), finite-difference time-domain (FDTD), parasitic patch, wide-band antennas.

I. INTRODUCTION

SINCE first introduced by Long *et al.* [1] in 1983, the dielectric resonator antenna (DRA) has received increasing attention in the last two decades. The DRA has many advantages such as its small size, low cost, low loss, light weight, and ease of excitation. It also has an advantage over the microstrip antenna in that the former has a wider impedance bandwidth.

The rectangular DRA has some advantages over the cylindrical and hemispherical DRAs. For example, by choosing proper dimensions of the rectangular DRA, the mode degeneracy problem can be avoided and, in addition, the bandwidth can be optimized [2].

In recent years, tremendous efforts have been paid on investigating the linearly polarized (LP) wide-band DRAs [3]–[26] and several methods have been proposed. The first one is to use more than one dielectric resonator (DR) elements [3]–[12], which is often called as a “stacked” DRA, with different sizes and/or dielectric materials. This method, however, will increase the antenna size and cost. The second approach is to use special-shaped DRAs [13]–[17], but these DRAs may not be easy to obtain commercially. Some feeding structures [18]–[26] can also be used to obtain a wide-band DRA.

In this paper, we will show that a dual-mode wide-band rectangular DRA can be obtained by just using a simple feeding

network, namely the strip-fed method. This method, which is compatible with the coaxial-probe version, can be found in [27], [28]. It has the distinct advantage over the coaxial probe counterpart in that it facilitates post manual trimmings.

Apart from the wide-band DRA, the circularly polarized (CP) DRA has also attracted tremendous research efforts [29]–[40] in recent years. Since a CP system is insensitive to the transmitter and receiver orientations, it finds a number of applications including satellite communication. Some CP DRAs were reported, which use either a quadrature feed [29], a single feed [30]–[32], or a tailor-made DRA [33]–[36]. Lately, a parasitic patch was placed on top of a rectangular DRA to generate CP fields [37], [38]. In that approach, the parasitic patch is located symmetrically on the top of the DRA. However, no information on the effect of the patch dimension and location on the CP characteristics were given. In this paper, the parasitic patch is placed on the side wall of the rectangular DRA. It is found that, as similar to the cylindrical and hemispherical DRA versions [39], [40], the CP characteristics are not very sensitive to the patch location and, hence, designing the CP DRA is not difficult.

In this work, the finite-difference time-domain (FDTD) method [41]–[43] is used to study the wide-band DRA as well as the CP DRA. To verify the calculations, measurements were carried out and, for each case, reasonable agreement between theory and experiment is obtained.

The organization of the paper is as follows. A strip-fed rectangular DRA with more than 40% bandwidth is studied in Section II. In Section III, a CP rectangular DRA with a parasitic patch is presented. Finally, a conclusion is drawn in Section IV.

II. WIDE-BAND LP ANTENNA WITHOUT PARASITIC PATCH

Usually more resonant modes are observed in a rectangular DRA compared to its cylindrical version over a normalized frequency range. This feature, in fact, can be used to enhance the bandwidth of the rectangular DRA if adjacent resonant modes have similar radiation patterns. For example, a truncated tetrahedron DRA [16] for wide-band applications has recently been realized using this concept.

Fig. 1 shows the geometry of a strip-fed rectangular DRA. The rectangular DRA has dimensions a , b , d and dielectric constant ϵ_r , whereas the feeding strip has length l_1 and width W_1 . The feeding strip is placed in the middle of the DRA side wall. Experimentally, the feeding strip was cut from an adhesive conducting tape and soldered to the inner conductor of a SMA connector. The DRA was put on an aluminum ground plane of size $30 \times 30 \text{ cm}^2$ ($\sim 6 \times 6 \lambda_0^2$ where λ_0 is the free-space wavelength at 6 GHz).

Manuscript received July 30, 2004; revised January 15, 2005. This work was supported by a grant from the Research Grant Council of the Hong Kong Special Administrative Region, China under Project: CityU 1178/01E.

The authors are with the Department of Electronic Engineering, City University of Hong Kong, Kowloon, Hong Kong (e-mail: eek-leung@mail.cityu.edu.hk).

Digital Object Identifier 10.1109/TAP.2005.850745

TABLE I
COMPARISON OF THE MEASURED FREQUENCIES, CALCULATED FREQUENCIES, AND PREDICTED FREQUENCIES OF THE DRA TE_{111}^y AND TE_{113}^y MODES

Resonant Modes	Measured resonant frequencies f_{mea} (GHz)	Calculated resonant frequencies (FDTD)		Predicted resonant frequencies (DWM)	
		f_{FDTD} (GHz)	error (%)	f_{DWM} (GHz)	error (%)
TE_{111}^y	3.81	3.90	2.3	3.74	-1.9
TE_{113}^y	4.57	4.60	0.7	4.55	-0.4

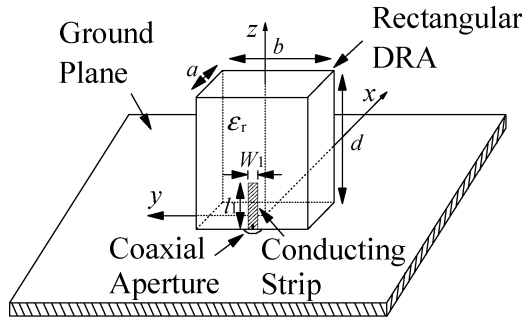


Fig. 1. Configuration of the strip-fed rectangular DRA.

The input impedance of a testing antenna of $a = 14.3$ mm, $b = 25.4$ mm, $d = 26.1$ mm, $l_1 = 10$ mm, $W_1 = 1$ mm, and $\epsilon_r = 9.8$ was measured using an HP8510C vector network analyzer, with the reference plane set at the coaxial aperture using the port extension. The previous conducting tape method [28] was used to remove any possible air gaps between the DRA and ground plane. To measure the radiation pattern of the antenna, the vector antenna measurement system HP8530A was used.

The above testing antenna can easily be simulated using the FDTD method with uniform Cartesian grid [41]. The space steps used in the FDTD simulation are $\Delta x = 0.715$ mm, $\Delta y = 0.508$ mm, and $\Delta z = 0.5$ mm. All of them are smaller than $\lambda_{\text{min}}/20$, where λ_{min} is the minimum operating dielectric wavelength. The time step satisfies the Courant stability condition [42]. A simple voltage-gap approximation is used to model the feed of the strip. A baseband Gaussian pulse is applied, with parameters $T = 0.083$ ns and $t_0 = 3T$. To terminate the boundary, a 10-cell-thick uniaxial perfectly matched layer (UPML) [43] absorber with polynomial spatial scaling ($m = 4$ and $\kappa_{\text{max}} = 1$) is used for all sides. In each direction, the distance from the rectangular DRA to the inner UPML interface is 20 space steps. The total grid size is $80\Delta x \times 110\Delta y \times 112\Delta z$, and $\sim 10\,000$ time steps are needed to allow the input response to vanish.

The calculated and measured input impedances are shown in Fig. 2, where reasonable agreement between theory and experiment is found. The corresponding $|S_{11}|$'s are shown in the inset of Fig. 2. It is found that the calculated and measured impedance bandwidths ($|S_{11}| < -10$ dB) of this antenna are 43% and 42%, respectively, which are much wider than that of the rectangular DRAs reported so far [21], [23], [26], [44], [45]. With reference to the inset, dual resonant TE_{111}^y and TE_{113}^y modes that broaden the antenna bandwidth can be observed clearly. Note that the TE_{112}^y mode cannot be found from the figure. To explain this, the mode patterns of the DRA TE_{111}^y , TE_{112}^y , and

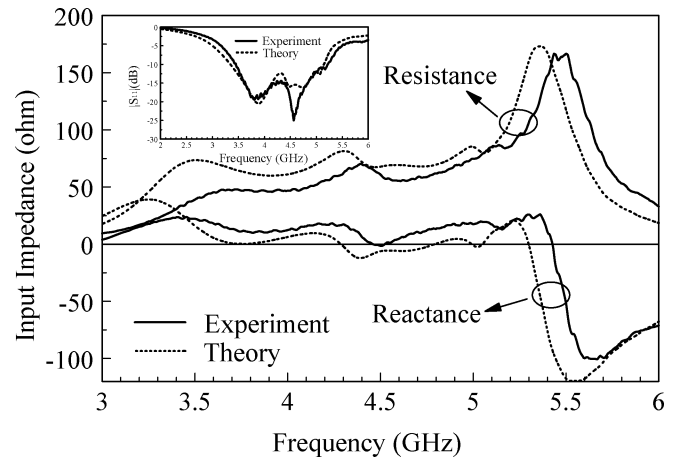


Fig. 2. Calculated and measured input impedances of the strip-fed rectangular DRA. The inset shows the calculated and measured $|S_{11}|$'s: $a = 14.3$ mm, $b = 25.4$ mm, $d = 26.1$ mm, $l_1 = 10$ mm, $W_1 = 1$ mm, and $\epsilon_r = 9.8$.

TE_{113}^y modes were studied. It was found that the H-field inside the DRA is very strong around the ground plane for both the TE_{111}^y and TE_{113}^y modes, but this is not the case for the TE_{112}^y mode. Since the strip current is maximum around the feed point for $l_1 \leq \lambda_g/4$ ($\lambda_g = \lambda_0/\sqrt{(\epsilon_r + 1)/2}$), only the TE_{111}^y and TE_{113}^y modes can be excited efficiently by our strip. It was found that when the strip length l_1 increases to about $\lambda_g/2$, it will be easier to observe the TE_{112}^y mode. From the field patterns, it was observed that some E_y component is generated inside the DRA due to the feeding strip. This makes the excited mode not a pure TE^y mode, but instead a pseudo- TE^y mode. Apart from the measured and calculated results, the resonant frequencies were also studied using the dielectric waveguide model (DWM), whose theory is given in the Appendix. Table I compares the measured resonant frequencies, calculated resonant frequencies using the FDTD method, and predicted resonant frequencies using the DWM model. Reasonable agreement between the results is obtained.

To ensure that the proposed DRA is a usable wide-band antenna, its radiation patterns are calculated and measured at the two TE_{111}^y - and TE_{113}^y -mode frequencies. The results are shown in Fig. 3. Again, reasonable agreement between theory and experiment is observed. From the figure, it is found that the broadside radiation patterns of the two resonant modes are very similar to each other, which is desirable. Since the antenna structure is symmetrical with respect to the xz plane, the calculated H (yz)-plane patterns are symmetrical. It is noted that the cross-polarization level of the higher-order TE_{113}^y mode

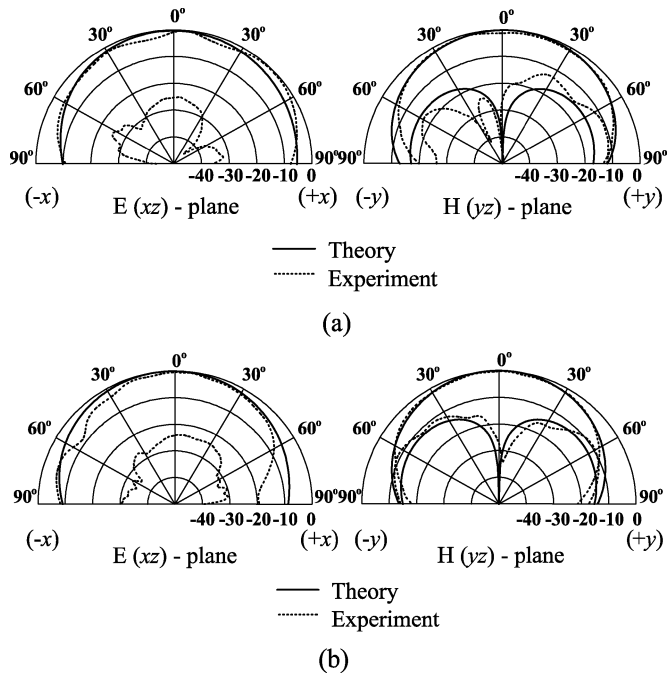


Fig. 3. Calculated and measured radiation patterns of the TE_{111}^y and TE_{113}^y modes. The parameters are the same as in Fig. 2. (a) TE_{111}^y mode ($f = 3.5$ GHz) and (b) TE_{113}^y mode ($f = 4.3$ GHz).

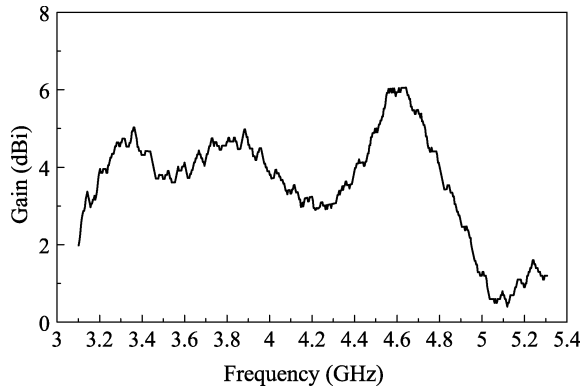


Fig. 4. Measured antenna gain as a function of frequency. The parameters are the same as in Fig. 2.

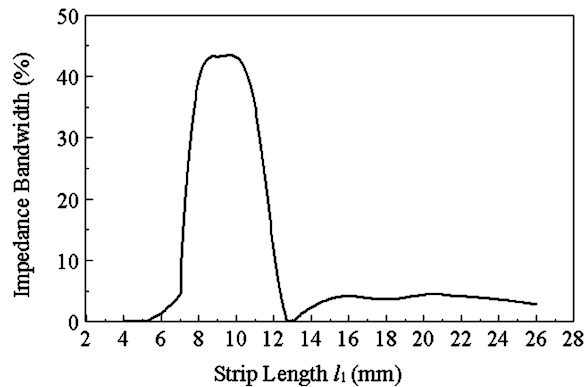


Fig. 5. Calculated impedance bandwidth as a function of strip length l_1 . Other parameters are the same as in Fig. 2.

is higher than that of the fundamental TE_{111}^y mode, which is to be expected. It is worth mentioning that theoretically,

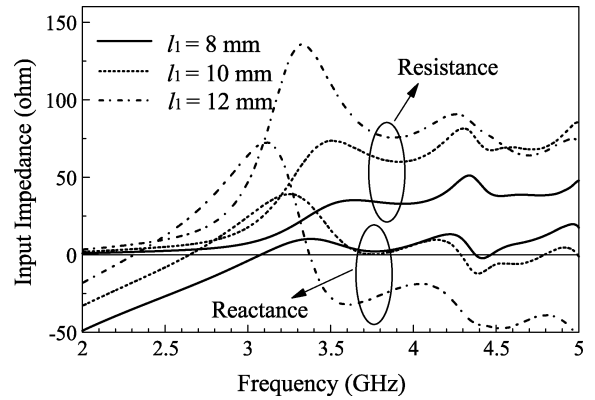


Fig. 6. Calculated input impedance as a function of frequency for $l_1 = 8, 10,$ and 12 mm. Other parameters are the same as in Fig. 2.

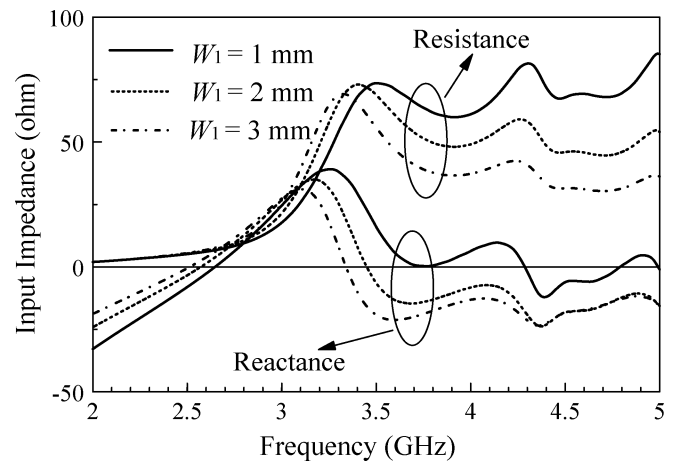


Fig. 7. Calculated input impedance as a function of frequency for $W_1 = 1, 2,$ and 3 mm. Other parameters are the same as in Fig. 2.

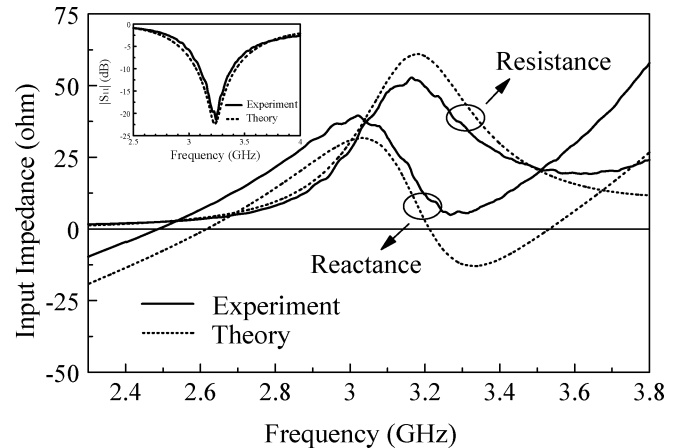


Fig. 8. Calculated and measured input impedances of a rectangular DRA. The inset shows the calculated and measured $|S_{11}|$'s: $a = 24$ mm, $b = 23.5$ mm, $d = 12.34$ mm, $l_1 = 10$ mm, $W_1 = 1$ mm, and $\epsilon_r = 9.5$.

there are no cross-polarized fields in the E-plane for an infinite ground plane, and the finite measured cross-polarized fields in that plane are caused by the measurement imperfection including the finite ground plane diffraction. The antenna gain of the configuration was measured and the result is shown in Fig. 4, where the 3-dB gain bandwidth is found to be 44%

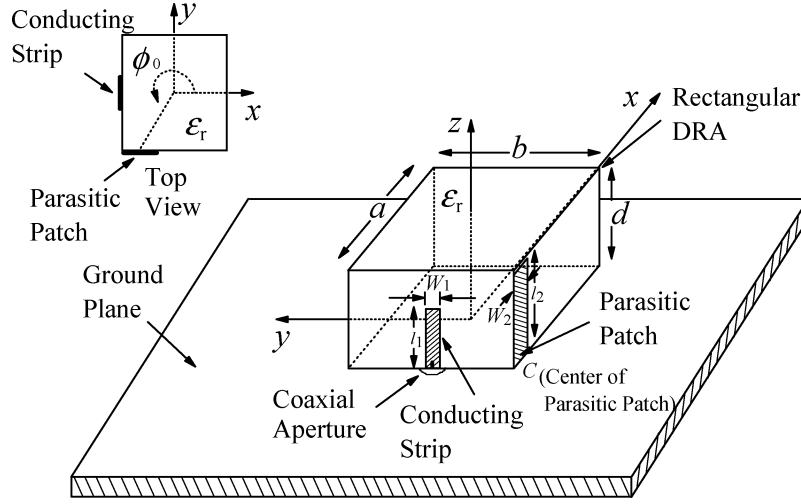


Fig. 9. Configuration of the strip-fed CP rectangular DRA with a parasitic patch.

(3.13–4.88 GHz). To overlap with the impedance bandwidth (3.45–5.22 GHz), the gain bandwidth is reduced to 34%.

The strip length l_1 is the major design parameter of the antenna. The calculated impedance bandwidth as a function of l_1 is shown in Fig. 5, where it is seen that a wide impedance bandwidth (>30%) can be obtained for the range $8 \leq l_1 \leq 11$ mm, in which the length l_1 is around $\lambda_g/4$ at the mid-band frequency (4.25 GHz).

The calculated input impedances for $l_1 = 8, 10,$ and 12 mm are shown in Fig. 6. As can be observed from the figure, the strip length l_1 can be adjusted to match the impedance. The results are similar to those obtained in the previous hemispherical-DRA version [28]. Fig. 7 shows the calculated input impedances for $W_1 = 1, 2,$ and 3 mm. It is observed that the strip width W_1 can also be used to tune the impedance, although it plays a secondary role only.

A wide impedance bandwidth can be obtained only when the height of the rectangular DRA is high enough. To demonstrate this, the same feeding structure was used on a low-height rectangular DRA with $a = 24$ mm, $b = 23.5$ mm, $d = 12.34$ mm, $l_1 = 10$ mm, $W_1 = 1$ mm, and $\epsilon_r = 9.5$. The measured and calculated input impedances and $|S_{11}|$'s are shown in Fig. 8, where only the fundamental TE_{111}^y mode is found in this case. The calculated and measured impedance bandwidths are 10% and 9%, respectively, with no bandwidth enhancement.

III. CP ANTENNA WITH PARASITIC PATCH

In this section, we study the strip-fed rectangular DRA with a parasitic patch for CP applications, with the configuration shown in Fig. 9. The narrowband DRA in the previous section is used again here. The rectangular DRA of dimensions $a = 24$ mm, $b = 23.5$ mm, $d = 12.34$ mm and dielectric constant $\epsilon_r = 9.5$ is fed by a conducting strip of length $l_1 = 10$ mm and width $W_1 = 1$ mm, which is attached at the center of the rectangular DRA side wall and soldered to the inner conductor of a SMA connector. A parasitic patch of length $l_2 = 12$ mm and width $W_2 = 1$ mm is attached to a DRA side wall at $\phi_0 = 225.6^\circ$, where ϕ_0 is the angle between the

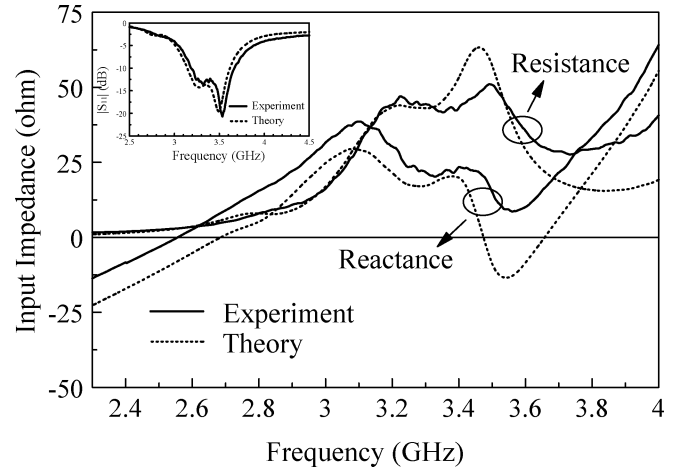


Fig. 10. Calculated and measured input impedances of the CP rectangular DRA. The inset shows the calculated and measured $|S_{11}|$'s: $a = 24$ mm, $b = 23.5$ mm, $d = 12.34$ mm, $l_1 = 10$ mm, $W_1 = 1$ mm, $l_2 = 12$ mm, $W_2 = 1$ mm, and $\epsilon_r = 9.5$.

x axis and the center of the parasitic patch. The uniform grid FDTD method [41] is used again in this section, with space steps $\Delta x = 0.5$ mm, $\Delta y = 0.49$ mm, and $\Delta z = 0.5$ mm, which are smaller than $\lambda_{\min}/20$. A simple voltage-gap model is used to simulate the feeding strip. A baseband Gaussian pulse with parameters $T = 0.083$ ns and $t_0 = 3T$ is used. The Courant stability condition and the previous UPML absorbing boundary condition are used again in this section. About 20 space steps between the rectangular DRA and the UPML are necessary in each direction. The overall grid size is $108\Delta x \times 108\Delta y \times 84\Delta z$, and ~ 15000 time steps are required in this case.

Fig. 10 shows the calculated and measured input impedances, and reasonable agreement between theory and experiment is obtained. The calculated and measured $|S_{11}|$'s are shown in the inset, where only the fundamental TE_{111}^y mode can be excited with this DRA. There are two resonant modes. The first resonance is caused by the strip-loaded DR mode, whereas the second one is caused by the patch-loaded DR mode. With reference to Fig. 10, the calculated and measured impedance bandwidths ($|S_{11}| < -10$ dB) are 14% and 14.5%, respectively.

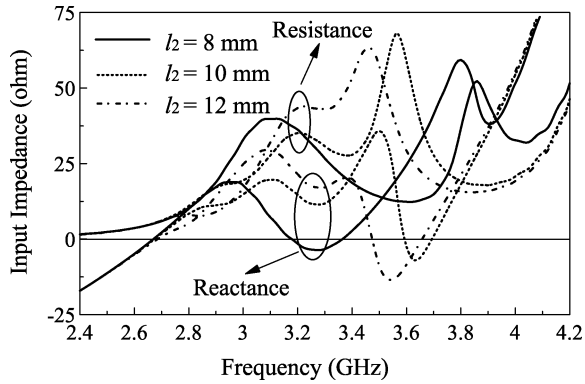


Fig. 11. Calculated input impedance as a function of frequency for parasitic patch length $l_2 = 8, 10,$ and 12 mm. Other parameters are the same as in Fig. 10.

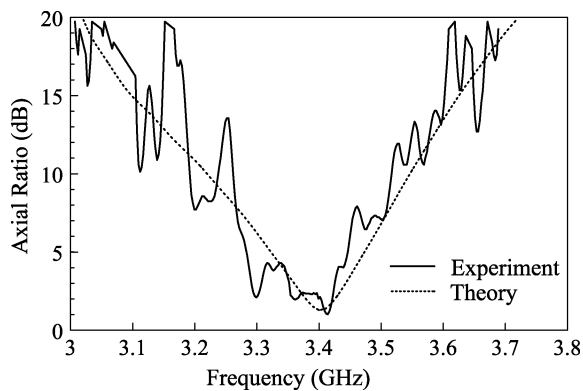


Fig. 12. Calculated and measured axial ratios as a function of frequency. The parameters are the same as in Fig. 10.

The effects of parasitic patch length l_2 on the input impedance are shown in Fig. 11. With reference to the figure, l_2 affects the impedance level of the antenna. The effect of the patch width W_2 on the input impedance was also studied. It was found that W_2 has only little effect on it. When $l_2 = 8$ mm, the patch-loaded DR mode and the strip-loaded DR mode are totally separated and can therefore be distinguished easily. As l_2 increases, the patch-loaded DR mode resonates at a lower frequency and consequently, it gets closer to the strip-loaded DR mode.

Fig. 12 shows the calculated and measured axial ratios (ARs) in the boresight direction ($\theta = 0^\circ$). The calculated AR is minimum at $f = 3.4$ GHz. It is found that the calculated 3-dB AR bandwidth is $\sim 2.7\%$, which is a typical value for a singly-fed CP DRA. The calculated and measured $x - z$ and $y - z$ plane radiation patterns at $f = 3.4$ GHz are displayed in Fig. 13, where a broadside radiation mode is observed. For each radiation plane, the left-hand circularly polarized (LHCP) field is more than 20 dB stronger than the right-hand circularly polarized (RHCP) field in the boresight direction. The antenna gain was measured. A conventional DRA gain curve with only one peak was obtained. The maximum gain was found to be 5.7 dBi.

Apart from the parasitic patch length l_2 , it is also important to study the effect of the feeding strip length l_1 on the CP design. Fig. 14 shows the calculated $|S_{11}|$ and AR for $l_1 = 8, 10,$ and 12 mm. As can be observed from the figure, the input impedance will change substantially with l_1 . However, the AR is almost unchanged for different l_1 's. Therefore, the strip length l_1 can be

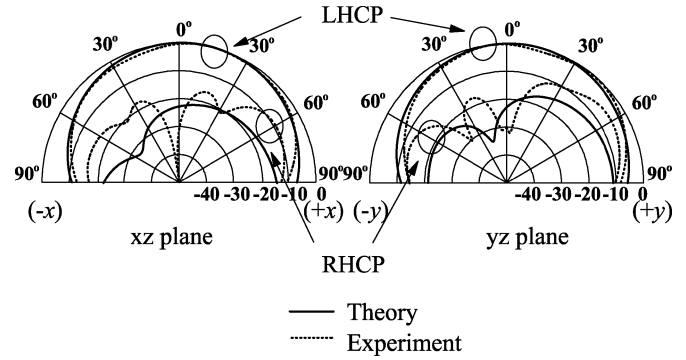


Fig. 13. Calculated and measured radiation patterns at $f = 3.4$ GHz. The parameters are the same as in Fig. 10.

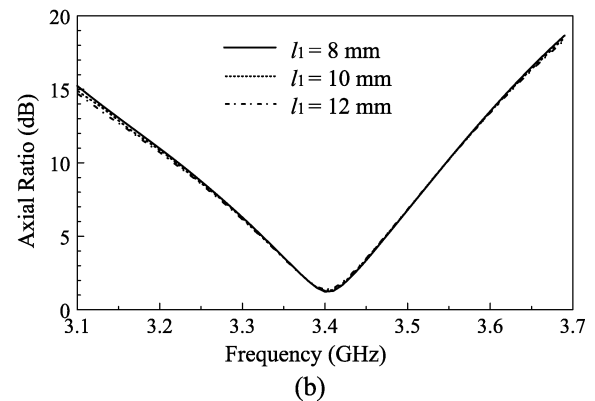
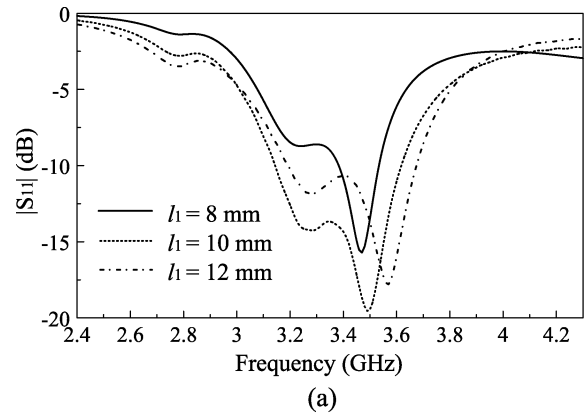


Fig. 14. Calculated $|S_{11}|$ and axial ratio as a function of frequency for $l_1 = 8, 10,$ and 12 mm. Other parameters are the same as in Fig. 10. (a) $|S_{11}|$ and (b) axial ratio.

adjusted to match the impedance with negligible changes on the AR. Again, the effects of strip width W_1 on the input impedance and AR were also studied. It was found that the effects are very small as compare with the strip length l_1 .

The minimum-AR value and its corresponding frequency versus the parasitic patch length l_2 are shown in Fig. 15. As l_2 increases, the minimum-AR value fluctuates whereas the corresponding frequency decreases monotonically. With reference to the figure, good ARs can be obtained around $l_2 = 9$ and 12 mm, showing that a CP design is not difficult to obtain. For each case, impedance match can be achieved by tuning the feeding strip length l_1 with virtually no effects on the AR, as discussed previously. Fig. 16 shows the effect of W_2 . Both the minimum-AR value and its corresponding frequency

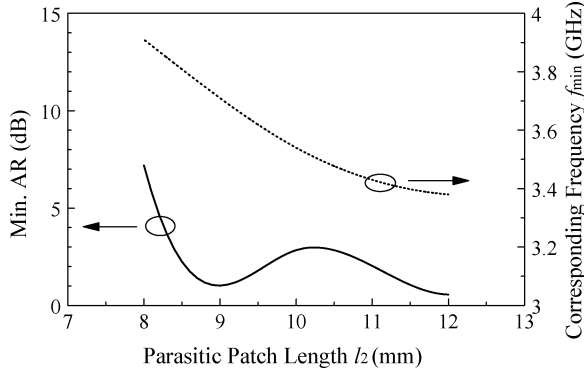


Fig. 15. Minimum axial ratio and its frequency as a function of parasitic patch length l_2 . Other parameters are the same as in Fig. 10.

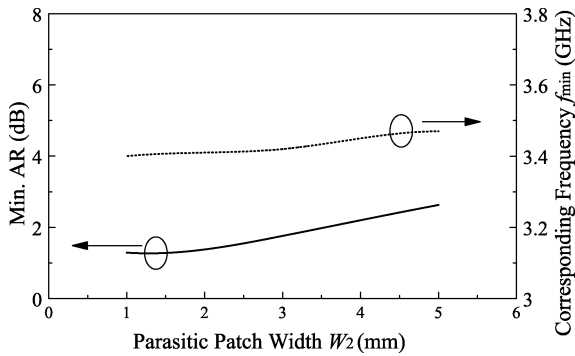


Fig. 16. Minimum axial ratio and its frequency as a function of parasitic patch width W_2 . Other parameters are the same as in Fig. 10.

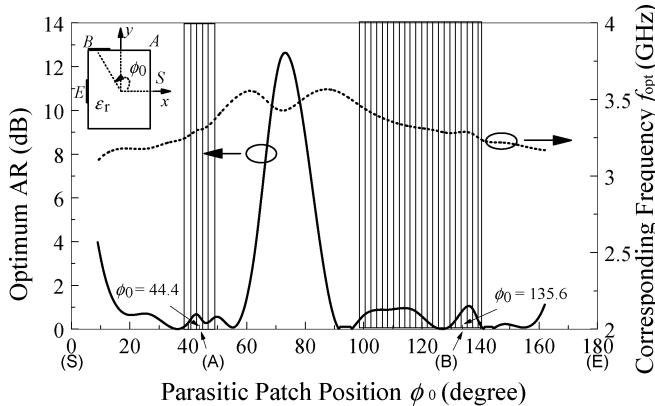


Fig. 17. Calculated optimum AR and its frequency f_{opt} as a function of parasitic patch position ϕ_0 . The shadow areas show the regions where $|S_{11}| < -10$ dB.

increase slightly with W_2 . It is interesting to note from Figs. 11 and 15 that the minimum-AR frequency follows the resonant frequency of patch-loaded DR mode.

The effect of patch location on the CP design is also studied, with the result shown in Fig. 17. Some important points are marked in the inset, which are S($\phi_0 = 0^\circ$), A($\phi_0 = 44.4^\circ$), B($\phi_0 = 135.6^\circ$), and E($\phi_0 = 180^\circ$). Since the antenna is symmetrical, only half ($\phi_0 = 0^\circ \sim 180^\circ$) of the angular range is considered. For each optimum AR, the parasitic patch length l_2 was tuned first to obtain a minimum AR, and then the feeding

strip length l_1 was adjusted to match the impedance. It can be seen from the figure that $\sim 60\%$ of the patch positions will give $AR < 1$ dB. The shadow regions of the figure are impedance passbands ($|S_{11}| < -10$ dB) of the antenna. The result shows that the parasitic patch should be placed around a corner of the rectangular DRA in order to obtain a good CP DRA. To match the impedance easier, we should choose the corner which is close to the feeding strip. Finally, it is observed from the dotted line of the figure that the operating frequency can be tuned by changing the location of the parasitic patch.

IV. CONCLUSION

The strip-fed excitation method has been applied to the rectangular DRA. A wide-band LP rectangular DRA has been studied first, which has been followed by a CP DRA with a parasitic patch. In the analysis, the uniform grid FDTD method has been used to find the input impedance and radiation field. For the LP antenna, the broadside fundamental TE_{111}^y mode and the higher order TE_{113}^y mode have been excited to obtain a wide impedance bandwidth of 43%. Of course, the low radiation Q-factor that can be achieved with the low dielectric constant has contributed to the wide-band result. For the CP part, it has been found that a parasitic patch can be used to design a CP rectangular DRA easily. For each of the LP and CP cases, measurements were carried out to verify the calculations, and reasonable agreement between theory and experiment has been obtained.

Finally, although the strips would add conduction losses to the antenna, the antenna efficiency should be significantly higher than that of the microstrip antenna, especially at millimeter-wave frequencies where the skin effect is strong.

APPENDIX

Mongia [46] has studied some higher order modes of a rectangular DR using the dielectric waveguide model (DWM) method. Using the DWM model, the TE_{mnl}^y -mode resonant frequency f_0 of the DRA can be given as follows:

$$f_0 = \frac{c}{2\pi\sqrt{\epsilon_r}} \sqrt{k_x^2 + k_y^2 + k_z^2} \quad (1)$$

where

$$k_x = \frac{m\pi}{a}, \quad k_z = \frac{l\pi}{2d} \quad (2)$$

$$k_y \tan\left(\frac{k_y b}{2}\right) = \sqrt{(\epsilon_r - 1)k_0^2 - k_y^2} \quad (\text{for } n = 1) \quad (3)$$

in which k_0 is the free-space wavenumber, c is the speed of light in vacuum, and k_x , k_y and k_z are wavenumbers inside the DR in the three directions, with $k_x^2 + k_y^2 + k_z^2 = \epsilon_r k_0^2$. The subscripts m , n , l of TE_{mnl}^y denote the number of extremes in the x , y , and z directions, respectively.

ACKNOWLEDGMENT

The authors gratefully appreciate the useful comments of the reviewers.

REFERENCES

- [1] S. A. Long, M. W. McAllister, and L. C. Shen, "The resonant cylindrical dielectric cavity antenna," *IEEE Trans. Antennas Propag.*, vol. 31, no. 5, pp. 406–412, May 1983.
- [2] R. K. Mongia and A. Ittipiboon, "Theoretical and experimental investigations on rectangular dielectric resonator antennas," *IEEE Trans. Antennas Propag.*, vol. 45, no. 9, pp. 1348–1356, Sep. 1997.
- [3] A. Petosa, N. Simons, R. Shiusansian, A. Ittipiboon, and M. Cuhaci, "Design and analysis of multisegment dielectric resonator antennas," *IEEE Trans. Antennas Propag.*, vol. 48, no. 5, pp. 738–742, May 2000.
- [4] A. A. Kishk, B. Ahn, and D. Kajfez, "Broadband stacked dielectric resonator antennas," *Electron. Lett.*, vol. 25, no. 18, pp. 1232–1233, Aug. 1989.
- [5] S. M. Shum and K. M. Luk, "Stacked annular ring dielectric resonator antenna excited by axi-symmetric coaxial probe," *IEEE Trans. Antennas Propag.*, vol. 43, no. 8, pp. 889–892, Aug. 1995.
- [6] A. A. Kishk, X. Zhang, A. W. Glisson, and D. Kajfez, "Numerical analysis of stacked dielectric resonator antennas excited by a coaxial probe for wideband applications," *IEEE Trans. Antennas Propag.*, vol. 51, no. 8, pp. 1996–2006, Aug. 2003.
- [7] R. Chair, A. A. Kishk, K. F. Lee, and C. E. Smith, "Wideband flipped staired pyramid dielectric resonator antennas," *Electron. Lett.*, vol. 40, no. 10, pp. 581–582, May 2004.
- [8] —, "Broadband aperture coupled flipped staired pyramid and conical dielectric resonator antennas," in *IEEE Antennas and Propagation Soc. Int. Symp. Dig.*, vol. 2, Monterey, CA, Jun. 2004, pp. 1375–1378.
- [9] M. Al Sharkawy, A. Z. Elsherbeni, and C. E. Smith, "Stacked elliptical dielectric resonator antennas for wide-band applications," in *IEEE Antennas and Propagation Soc. Int. Symp. Dig.*, vol. 2, Monterey, CA, Jun. 2004, pp. 1371–1374.
- [10] K. W. Leung, K. Y. Chow, K. M. Luk, and E. K. N. Yung, "Offset dual-disk dielectric resonator antenna of very high permittivity," *Electron. Lett.*, vol. 32, pp. 2038–2039, Oct. 1996.
- [11] K. W. Leung, K. M. Luk, K. Y. Chow, and E. K. N. Yung, "Bandwidth enhancement of dielectric resonator antenna by loading a low-profile dielectric disk of very high permittivity," *Electron. Lett.*, vol. 33, pp. 725–726, Apr. 1997.
- [12] S. H. Ong, A. A. Kishk, and A. W. Glisson, "Wideband disk-ring dielectric resonator antenna," *Microwave Opt. Tech. Lett.*, vol. 35, pp. 425–428, Dec. 2002.
- [13] A. Ittipiboon, A. Petosa, D. Roscoe, and M. Cuhaci, "An investigation of a novel broadband dielectric resonator antenna," in *IEEE Antennas and Propagation Soc. Int. Symp. Dig.*, vol. 3, Baltimore, MA, Jul. 1996, pp. 2038–2041.
- [14] A. A. Kishk, A. W. Glisson, and G. P. Junker, "Bandwidth enhancement for split cylindrical dielectric resonator antennas," *Progress In Electromagnetic Research*, vol. 33, pp. 97–118, 2001.
- [15] A. A. Kishk, Y. Yin, and A. W. Glisson, "Conical dielectric resonator antennas for wide-band applications," *IEEE Trans. Antennas Propag.*, vol. 50, no. 4, pp. 469–474, Apr. 2002.
- [16] A. A. Kishk, "Wide-band truncated tetrahedron dielectric resonator antenna excited by a coaxial probe," *IEEE Trans. Antennas Propag.*, vol. 51, no. 10, pp. 2913–2917, Oct. 2003.
- [17] K. Pliakostathis and D. Mirshekar-Syahkal, "Stepped dielectric resonator antennas for wide-band applications," in *IEEE Antennas and Propagation Soc. Int. Symp. Dig.*, vol. 2, Monterey, CA, Jun. 2004, pp. 1367–1370.
- [18] K. W. Leung, W. C. Wong, K. M. Luk, and E. K. N. Yung, "Annular slot-coupled dielectric resonator antenna," *Electron. Lett.*, vol. 34, pp. 1275–1277, Jun. 1998.
- [19] K. W. Leung, H. Y. Lo, K. K. So, and K. M. Luk, "High-permittivity dielectric resonator antenna excited by a rectangular waveguide," *Microw. Opt. Techn. Lett.*, vol. 34, no. 3, pp. 157–158, Aug. 2002.
- [20] K. W. Leung and C. K. Leung, "Wideband dielectric resonator antenna excited by cavity-backed circular aperture with microstrip tuning fork," *Electron. Lett.*, vol. 39, pp. 1033–1035, Jul. 2003.
- [21] O. Kivekas, J. Ollikainen, and P. Vainikainen, "Wideband dielectric resonator antenna for mobile phones," *Microwave Opt. Tech. Lett.*, vol. 36, no. 1, pp. 25–26, Jan. 2003.
- [22] S. K. Menon, B. Lethakumary, P. Mohanan, P. V. Bijumon, and M. T. Sebastian, "Wideband cylindrical dielectric resonator antenna excited using an L-strip feed," *Microwave Opt. Tech. Lett.*, vol. 42, no. 4, pp. 293–294, Aug. 2004.
- [23] S. Mridula, B. Paul, S. K. Menon, C. K. Aanandan, K. Vasudevan, P. Mohanan, P. V. Bijumon, and M. T. Sebastian, "Wideband rectangular dielectric resonator antenna for W-Lan applications," in *IEEE Antennas and Propagation Soc. Int. Symp. Dig.*, vol. 2, Monterey, CA, Jun. 2004, pp. 1363–1366.
- [24] K. M. Luk, M. T. Lee, K. W. Leung, and E. K. N. Yung, "Technique for improving coupling between microstripline and dielectric resonator antenna," *Electron. Lett.*, vol. 35, pp. 357–358, Mar. 1999.
- [25] Y. X. Guo and K. M. Luk, "On improving coupling between a coplanar waveguide feed and a dielectric resonator antenna," *IEEE Trans. Antennas Propag.*, vol. 51, no. 8, pp. 2144–2146, Aug. 2003.
- [26] G. Bit-Babik, C. Di Nallo, and A. Faraone, "Multimode dielectric resonator antenna of very high permittivity," in *IEEE Antennas and Propagation Soc. Int. Symp. Dig.*, vol. 2, Monterey, CA, Jun. 2004, pp. 1383–1386.
- [27] M. Copper, "Investigation of current and novel rectangular dielectric resonator antennas for broadband applications at L-band frequencies," Master's thesis, Carleton Univ., Northfield, MN, 1997.
- [28] K. W. Leung, "Conformal strip excitation of dielectric resonator antenna," *IEEE Trans. Antennas Propag.*, vol. 48, no. 6, pp. 961–967, Jun. 2000.
- [29] K. W. Leung, W. C. Wong, K. M. Luk, and E. K. N. Yung, "Circular-polarized dielectric resonator antenna excited by dual conformal strips," *Electron. Lett.*, vol. 36, pp. 484–486, Mar. 2000.
- [30] C. Y. Huang, J. Y. Wu, and K. L. Wong, "Cross-slot-coupled microstrip antenna and dielectric resonator antenna for circular polarization," *IEEE Trans. Antennas and Propag.*, vol. 47, no. 4, pp. 605–609, Apr. 1999.
- [31] K. W. Leung and S. K. Mok, "Circularly polarized dielectric resonator antenna excited by perturbed annular slot with backing cavity," *Electron. Lett.*, vol. 37, pp. 934–936, Jul. 2001.
- [32] B. Li, K. K. So, and K. W. Leung, "A circularly polarized dielectric resonator antenna excited by an asymmetrical U-slot with a backing cavity," *IEEE Antennas Wireless Propag. Lett.*, vol. 2, pp. 133–135, 2003.
- [33] M. B. Oliver, Y. M. M. Antar, R. K. Mongia, and A. Ittipiboon, "Circularly polarized rectangular dielectric resonator antenna," *Electron. Lett.*, vol. 31, pp. 418–419, Mar. 1995.
- [34] M. T. K. Tam and R. D. Murch, "Circularly polarized circular sector dielectric resonator antenna," *IEEE Trans. Antennas Propag.*, vol. 48, no. 1, pp. 126–128, Jan. 2000.
- [35] A. A. Kishk, "Performance of planar four-element array of single-fed circularly polarized dielectric resonator antenna," *Microwave Opt. Tech. Lett.*, vol. 38, no. 5, pp. 381–384, Sep. 2003.
- [36] —, "An elliptic dielectric resonator antenna designed for circular polarization with single feed," *Microwave Opt. Tech. Lett.*, vol. 37, no. 6, pp. 454–456, June 2003.
- [37] F. R. Hsiao, T. W. Chiou, and K. L. Wong, "Circularly polarized low-profile square dielectric resonator antenna with a loading patch," *Microwave Opt. Tech. Lett.*, vol. 31, pp. 157–159, Nov. 2001.
- [38] A. Laisné, R. Gillard, and G. Piton, "Circularly polarized dielectric resonator antenna with metallic strip," *Electron. Lett.*, vol. 38, pp. 106–107, Jan. 2002.
- [39] K. W. Leung and H. K. Ng, "Theory and experiment of circularly polarized dielectric resonator antenna with a parasitic patch," *IEEE Trans. Antennas Propag.*, vol. 51, no. 3, pp. 405–412, Mar. 2003.
- [40] R. T. Long, R. J. Dorris, S. A. Long, M. A. Khayat, and J. T. Williams, "Use of parasitic strip to produce circular polarization and increased bandwidth for cylindrical dielectric resonator antenna," *Electron. Lett.*, vol. 37, pp. 406–408, Mar. 2001.
- [41] Y. S. Yee, "Numerical solution of initial boundary value problems involving Maxwell's equations in isotropic media," *IEEE Trans. Antennas Propag.*, vol. 14, no. 3, pp. 302–307, May 1966.
- [42] A. Taflov, *Computational Electrodynamics: The Finite Difference Time Domain Method*. Norwood, MA: Artech House, 2000.
- [43] S. D. Gedney, "An anisotropic perfectly matched layer-absorbing medium for the truncation of FDTD lattices," *IEEE Trans. Antennas and Propag.*, vol. 44, no. 12, pp. 1630–1639, Dec. 1996.
- [44] M. S. Al Salameh, Y. M. M. Antar, and G. Séguin, "Coplanar-waveguide-fed slot-coupled rectangular dielectric resonator antenna," *IEEE Trans. Antennas Propag.*, vol. 50, no. 10, pp. 1415–1419, Oct. 2002.
- [45] S. M. Shum and K. M. Luk, "Analysis of aperture coupled rectangular dielectric resonator antenna," *Electron. Lett.*, vol. 30, pp. 1726–1727, Oct. 1994.
- [46] R. K. Mongia, "Theoretical and experimental resonant frequencies of rectangular dielectric resonators," *Proc. Inst. Elect. Eng.*, vol. 139, pp. 98–104, Feb. 1992.



Bin Li (S'03) was born in Tianjin, China, in 1978. He received the B.Eng. degree in electronic engineering from Xidian University, Xi'an, China, in 2001. Currently, he is working toward the Ph.D. degree in the Department of Electronic Engineering, the City University of Hong Kong.

His current research interests include dielectric resonator antennas, microstrip antennas and numerical methods in electromagnetics.



Kwok Wa Leung (S'90–M'93–SM'02) was born in Hong Kong on April 11, 1967. He received the B.Sc. degree in electronics and the Ph.D. degree in electronic engineering from the Chinese University of Hong Kong, in 1990 and 1993, respectively.

From 1990 to 1993, he was a Graduate Assistant with the Department of Electronic Engineering, the Chinese University of Hong Kong. In 1994, he joined the Department of Electronic Engineering at City University of Hong Kong as an Assistant Professor and became an Associate Professor in 1999. From

2001 to 2004, he was appointed as the Programme Leader for the B.Eng. (Honors) in Electronic and Communication Engineering. His research interests include dielectric resonator antennas, microstrip antennas, wire antennas, numerical methods in electromagnetics, and mobile communications.

Dr. Leung received the URSI Young Scientists Awards in 1993 and 1995, awarded by XXIVth General Assembly of the International Union of Radio Science (URSI) and 15th URSI Triennial International Symposium on Electromagnetic Theory, respectively.